CPC(HEP & NP), 2011, **35**(1): 35–39 **Chinese Physics C** Vol. 35, No. 1, Jan., 2011

Theoretical analysis of double-differential neutron emission cross sections for n+^{56}Fe reactions at incident energies of 7–13 MeV[*]

HOU Pei-You(侯培友) SUN Xiao-Jun(孙小军)[1)] YU Cheng-Gang(余呈刚) LU Xiao(陆晓)

College of Physics and Technology, Guangxi Normal University, Guilin 541004, China

Abstract: The double-differential neutron emission cross sections for n+^{56}Fe reactions at incident energies of 7–13 MeV at different angles are calculated by the UNF (abbreviation for unified, 2009 Version) code, which is based on the unified Hauser-Feshbach and exciton model. The results indicate that the higher the incident energies, the better the results, although there are some discrepancies between the calculated results and the measured data for natural iron. These discrepancies are analyzed in detail in this paper. In addition, the calculated results are also compared with the evaluated results of ENDF/B Ⅶ.0 and JEFF-3.1.1 near the angle of 90° at incident energies of 8.17 and 11.5 MeV, respectively.

Key words: Unified Hauser-Feshbach and exciton model, double-differential neutron emission cross section, UNF

PACS: 25.10.+s, 28.20.Cz **DOI:** 10.1088/1674-1137/35/1/008

1 Introduction

Iron is the main structural material and is almost omnipresent in any nuclear power reactor. Data from neutron-induced reactions for iron, especially the double-differential neutron emission cross sections (DDXs), are of great significance in the development of nuclear energy and in nuclear engineering. For example, DDXs at incident energies of 7–13 MeV are very important for the neutronic design of fusion and fast reactors, as mentioned in Ref. [1]. Iron consists of the following isotopes (abundancies are given in the brackets): ^{54}Fe (5.845%), ^{56}Fe (91.754%), ^{57}Fe (2.119%) and ^{58}Fe (0.282%) [2]. So the evaluation must be performed on each isotope in order to obtain accurate DDXs for natural iron. However, the experimental DDXs for these isotopes are very scarce, especially below the incident energy of 20 MeV. Apart from the resonance range (resonance range is regarded generally for an incident energy range of $E_{\rm n} \lesssim 7$ MeV [3, 4]), there are only experimental DDXs for natural iron below 20 MeV. Therefore, the accurate evaluations of each isotope and natural iron are difficult in this range of incident energies. Thus the evaluation data of the highest abundant isotope ^{56}Fe are used generally as a reference [4].

Because of the lack of mono-energetic neutron sources and facilities, the DDX data for Fe isotopes and even for natural iron at incident energies of 7–13 MeV were lacking until the end of the 20th century. Although Beyerle et al measured the DDXs data for natural iron at incident neutron energies of 7.5, 10.0 and 12.0 MeV in 1979 [5], these data are not precise enough and their trends are not consistent with any theoretical predictions. In addition, the DDXs data for natural iron were measured by Biryukov et al. at an incident neutron energy of 9.1 MeV in 1974 [6], by Soda et al. at 11.5 MeV in 1995 [7], by Qi Bu-Jia et al. at 10.0 MeV in 1999 [8] and by Ruan Xi-Chao et al. at 8.17 MeV in 2009 [9]. These data will provide some proof of the reasonableness of reaction model used here.

For many years, a tremendous effort has been invested in theoretical models for neutron-induced reactions on isotopic or natural iron [10], but the calculated DDXs at incident energies of 7–13 MeV

Received 6 April 2010

[*] Supported by National Natural Science Foundation of China (10547005, 10975038), China Postdoctoral Science Foundation (20090450720) and Innovation Project of Guangxi Graduate Education (2009106020702M38)

1) E-mail: sxj0212@mailbox.gxnu.edu.cn

(except for the incident energy of 11.5 MeV [4]) have not been published until now. Many interpretations of the DDXs for iron (natural or isotopic) are based on data at incident energies of $E_{\rm n} \gtrsim 13$ MeV [1, 3, 4, 11–13], but cannot reasonably be extrapolated to the low-energy range. Based on the agreement with the experimental double-differential cross sections including neutrons, alphas and protons at incident energies of 13–20 MeV in our earlier work1), the model calculation reasonably extrapolates the incident neutron energies of 7–13 MeV considered in this paper.

This paper proceeds as follows. In Section 2, the theoretical model of the UNF code, such as the unified Hauser-Feshbach and exciton model, optical model and the potential parameters, is introduced. Our calculated DDXs are given and analyzed at incident energies of 8.17, 9.1, 10.0 and 11.5 MeV, respectively, in Section 3. A comparison with the results of some evaluated libraries, such as the ENDF/B-Ⅶ.0 and the JEFF-3.1.1, is also presented in this section. The summary is given in the last Section.

2 Theoretical model

Neutron-induced reactions on medium mass nuclei are different from those on light nuclei reactions, in which particle emissions between the discrete levels dominates the whole reaction process [14–17]. For the n+^{56}Fe (medium mass nucleus) reaction, contributions to the DDXs come mainly from transitions from continuum states to discrete levels, as well as from continuum states to continuum states. The unified Hauser-Feshbach and exciton model [18] is used to describe the nuclear reaction equilibrium and pre-equilibrium decay processes. The Hauser-Feshbach model with a width fluctuation correction describes the emissions from the compound nucleus to the discrete levels and continuum states of the residual nuclei in equilibrium processes, while the pre-equilibrium processes are described by the angular momentum dependent exciton model. The multi-particle emissions to the discrete levels and continuum states for all accessible channels are included. The formulae of the DDXs are given in Refs. [19] and [20], which give the cases of emissions to the discrete levels and the continuum states respectively. The exact Pauli exclusion effects and the Fermi motion of the nucleons in the exciton state densities [21] are taken into account. The partial wave coefficients of the single nucleon emission are calculated by the linear momentum dependent exciton state density model [22]. Thus, the recoil effects in the multi-particle emissions from continuum states to discrete levels, as well as from continuum states to continuum states, are also strictly taken into account so that the energy balance in every open reaction channel is exactly fulfilled.

The optical model is used to describe the measured neutron-induced total, non-elastic, elastic cross sections and elastic-scattering angular distributions, and to calculate the transmission coefficients of the compound nucleus and the pre-equilibrium emission process. The optical potential and a set of neutron optical potential parameters for ^{56}Fe are obtained by the APMN code [23], which takes the level schemes of target and the residual nuclei as input parameters and can automatically search the optimal optical potential parameters such as to fit fairly well with the relevant experimental total, nonelastic, elastic cross sections and elastic scattering angular distributions.

A new version of the theoretical model code UNF [20] was developed in 2009 based on the optical model and the unified Hauser-Feshbach and exciton model for incident neutron energies below 20 MeV. In addition, the direct inelastic-scattering cross sections and angular distributions of discrete levels for ^{56}Fe are precalculated by the distorted wave Born approximation theory (DWUCK4 code) [24]. The discrete levels are taken into account from the ground state up to the 39th (4.66^{2+}) excited state. Levels above the highest excited state are assumed to be overlapping and a level density formula is used. The precalculated direct inelastic scattering cross sections and angular distributions are entered into the UNF calculations.

3 Results and analysis

Since, as mentioned above, there are no experimental DDXs data for the target nuclide ^{56}Fe (with an abundancy of up to 91.754%) and incident neutron energies 7–13 MeV available, in this work we use the data of natural Fe to compare with the calculated results. This comparison for the incident energies of 8.17, 9.1, 10.0 and 11.5 MeV is as shown in Figs. 1–4, respectively. The results indicate that there are some fluctuations in both the experimental data and the theoretical calculations, especially at lower incident energies. It is obvious that these fluctuations, with peaks and valleys localized near the discrete levels of ^{56}Fe, mainly originate from the emission processes continuum states to discrete lev-

---

1) SUN Xiao-Jun, HOU Pei-You, QU Wen-Jing et al. Model Calculation of Neutron Kerma Coefficient for n+^{56}Fe Below 20 MeV, 2010.

els. For example, the right peak and valley apparently originate from the contributions of the ground states, the first excited level (0.8468 MeV) and the second excited level (2.0851 MeV). With increasing incident energies, the contributions of the continuum states to continuum states increase accordingly, so the fluctuations of the DDXs become smoother and the calculated results agree better with the experimental data.

As shown in Fig. 1, there is good agreement for outgoing energies $\lesssim$3 MeV and $\gtrsim$6 MeV, but between 3–6 MeV the calculated DDXs show some structure and even underestimate the experimental data. One reason is that the model calculation is only performed for the n+^{56}Fe reaction, which has specific discrete levels. However, the experimental DDXs data, derived from natural iron, are effected by the discrete levels of each isotope. So the experimental DDXs data are smooth especially at lower outgoing energies. The same happens at incident energies of 9.1 and 10.0 MeV as shown in Figs. 2 and 3. In addition, two larger abundant isotopes ^{54}Fe (5.845%) and ^{56}Fe (91.754%) are

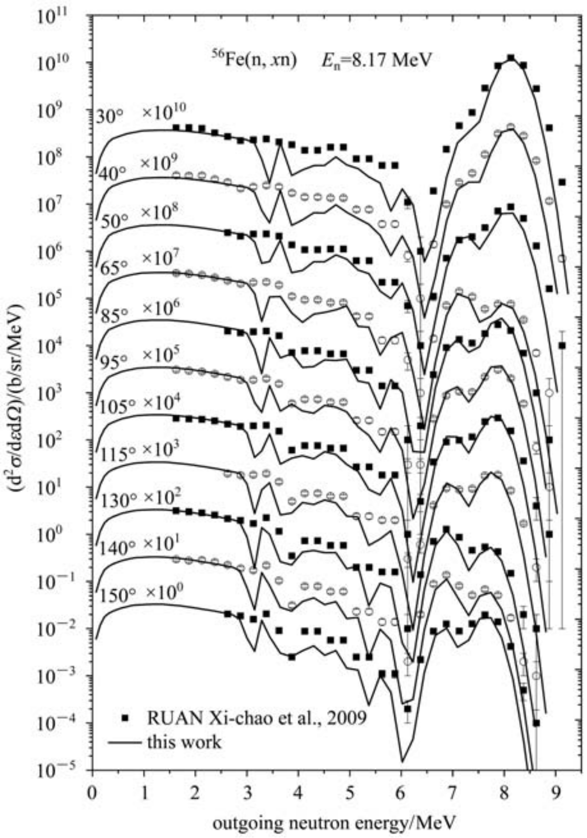

Fig. 1. Calculated DDXs of this work (solid line) vs outgoing neutron energies for different angles at an incident energy of 8.17 MeV on natural Fe. The measured data (symbols) are taken from Ref. [9].

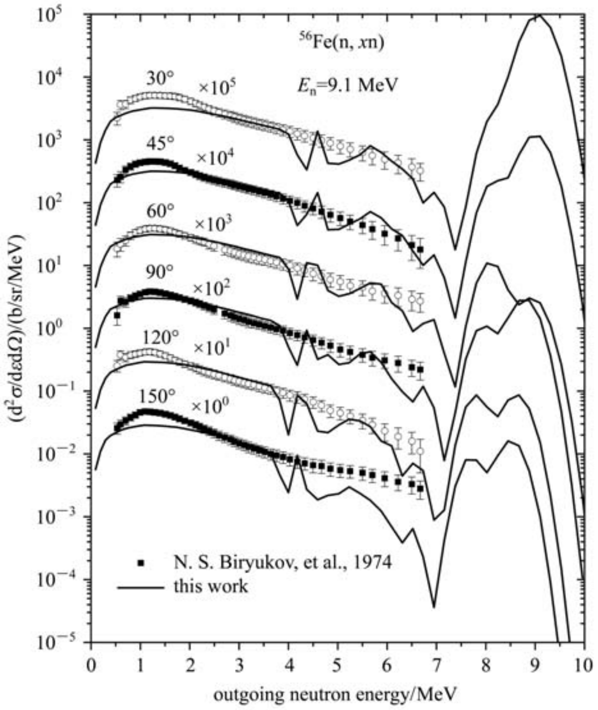

Fig. 2. Same as Fig. 1, but at 9.1 MeV. The measured data (symbols) are from Ref. [6].

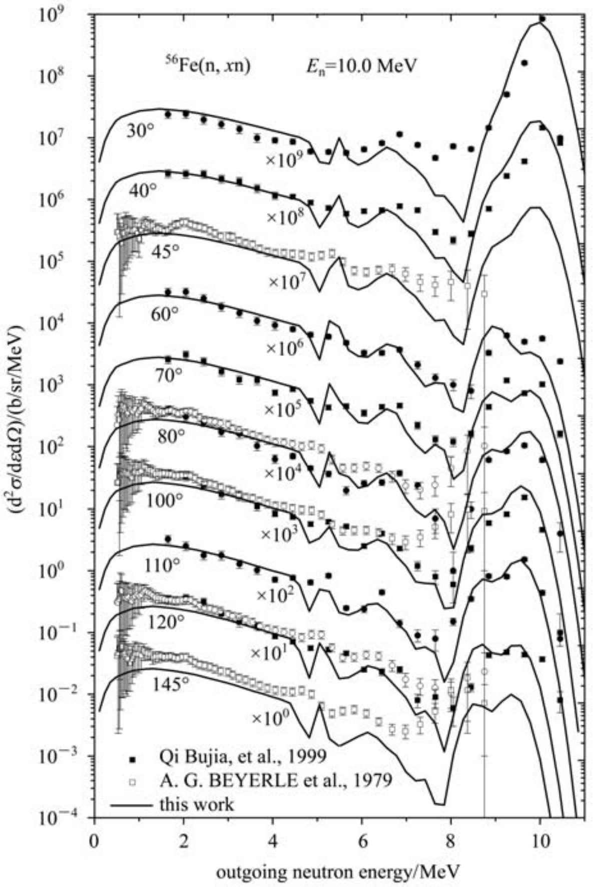

Fig. 3. Same as Fig. 1, but at 10.0 MeV. The measured data are from Ref. [8] (full symbols) and Ref. [5] (hollow symbols), respectively.

pf-shell nuclei at or near the closed $N=28$ neutron shell. Both isotopes have a yrast (2^+) level at ≈ 1 MeV and coulomb-excitation leads to β_2 values (≈ 0.24) for the primary ^{56}Fe isotope. This is a relatively large value and thus there are significant direct collective contributions [10]. Thus the collective neutron interactions with two isotopes are primarily with the proton core and these contributions are not considered by the UNF code.

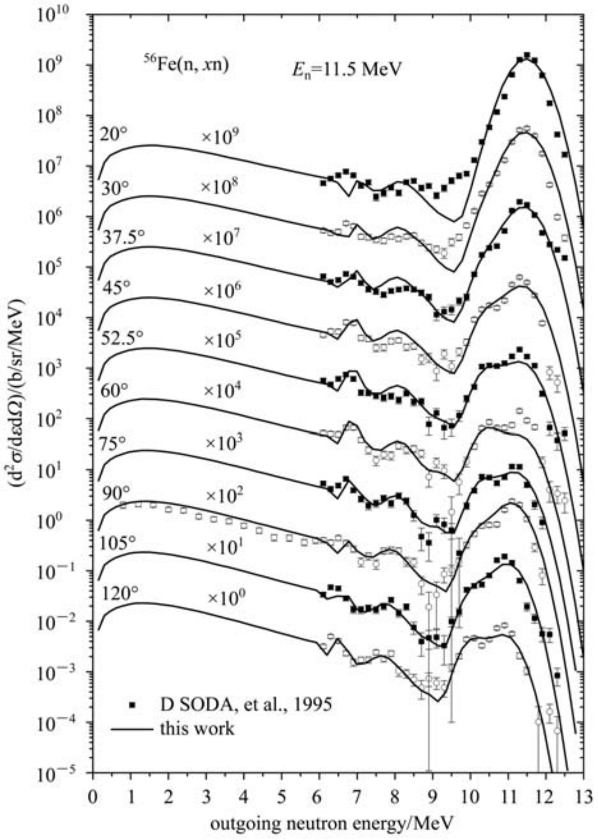

Fig. 4. Same as Fig. 1, but at 11.5 MeV. The measured data (symbols) are from Ref. [7].

Although the fluctuant DDXs of this model calculation appear at incident neutron energies of 8.17, 9.1, 10.0 and 11.5 MeV, the fluctuations weaken gradually with increasing incident energy, as shown in Figs. 1–4. At an incident energy of 10.0 MeV, the calculated DDXs agree well with the experimental data measured by Qi Bu-Jia et al. in 1999, although they are almost all at outgoing neutron energies lower than the experimental data measured by Beyerle in 1979 [5]. Furthermore, the calculated results are in good agreement with the experimental data at 11.5 MeV, as well as at incident energies 13–20 MeV as given in our earlier work.

The calculated DDXs of this paper are compared with the evaluated results of ENDF/B Ⅶ.0 (released in 2006) and JEFF-3.1.1 (released in 2009) near 90° angle at incident energies 8.17 and 11.5 MeV, respectively. As shown in Fig. 5, the results of the ENDF/B Ⅶ.0 (dash line) and the JEFF-3.1.1 (dot line) are almost identical, but their fluctuations are stronger than those of this work (solid line) at incident energies of 8.17 and 11.5 MeV. In addition, the recently evaluated DDXs from the RUSFOND (released in 2010) are only derived from the JEFF-3.1.1, so their results are no longer shown in this paper. As shown in Figs. 1-5, one can see that the calculated results in this paper are reasonable.

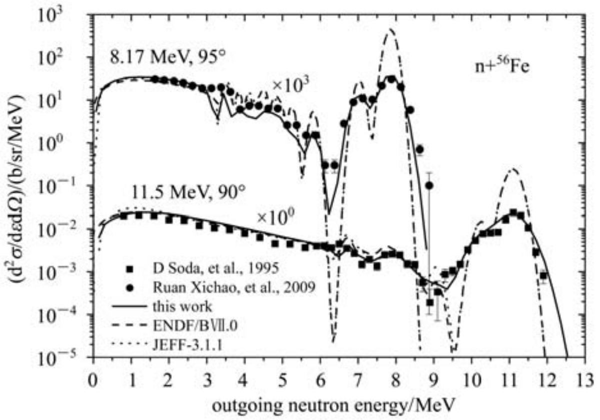

Fig. 5. Calculated DDXs of this paper compared with the measured data and the evaluated results near 90° angle at incident energies 8.17 and 11.5 MeV, respectively. The measured data are from Ref. [7] (full square) and Ref. [9] (full circle) respectively. The solid, dashed and dotted lines are the results of this paper, ENDF/B Ⅶ.0 and JEFF-3.1.1, respectively.

4 Summary

On the basis of the unified Hauser-Feshbach and exciton model, a model calculation using the UNF (2009 version) code is performed for a n+^{56}Fe reaction at incident energies of 7–13 MeV. The calculated DDXs of this paper refer to incident energies of 8.17, 9.1, 10.0 and 11.5 MeV for different angles. Some fluctuations of the DDXs in a certain outgoing neutron energy range are analyzed in detail. Although the results between the calculated DDXs and the experimental data for natural iron at incident energies of 8.17 and 9.1 MeV have some discrepancies, the trend is reasonable, improving with increasing incident neutron energy, as shown at 10.0 and 11.5 MeV, and even at the higher incident energies given in our earlier work. In order to verify the reasonableness of reaction model when applied to isotopic or natural iron, we hope that more experimental data for ^{56}Fe or other isotopes at low incident energies will be available in the future.

References

1 Matsuyama S, Soda D, Baba M et al. Measurements of Double-Differential Neutron Emission Cross Sections of Fe and Nb for 11.5 MeV Neutrons. In: Masayoshi K, Tokio F ed. Proceedings of the 1994 Symposium on Nuclear Data. Tokai: Japan Atomic Energy Research Institute. 1995. 157

2 Tuli J K. Nuclear Wallet Cards. New York: National Nuclear Data Center, 2005. 11

3 Duijvestijn M C, Koning A J. Annals of Nuclear Energy, 2006, **33**: 1196

4 HAN Yin-Lu, ZHANG Yue, GUO Hai-Rui. Nucl. Sci. Eng, 2009, **161**: 1

5 Beyerle A G, Gould C, Seagondollar W et al. Double Differential Neutron Scattering Cross Sections for Fe, Cu, Ni and Pb Between 8 and 12 MeV. In: Fowler J L, Johnson C H, Bowman C D ed. Proceedings of the International Conference. Knoxville: US Department of Commerce National Bureau of Standards. 1980. 139

6 Biryukov N S, Zhuravlev B V, Kornilov N V et al. Yad.Fiz., 1974, **19**(6): 1190

7 Soda D, Matsuyama S, Masanobu I et al. Report of Japan Atomic Energy Research Institute, 1995, Report No. JAERI-M-96-008

8 QI Bu-Jia, TANG Hong-Qing, ZHOU Zu-Ying et al. Atomic Energy Science and Technology, 1999, **33**(6): 497 (in Chinese)

9 RUAN Xi-Chao, HUANG Han-Xiong, JIANG Jing et al. Atomic Energy Science and Technology, 2009, **43**(9): 793 (in Chinese)

10 Smith A B. Nuclear Physics A, 1996, **605**: 269

11 HAN Yin-Lu, ZHANG Yue, GOU Hai-Rui et al. Annals of Nuclear Energy, 2008, **35**: 2031

12 Gul K, Anwar M, Ahmad M et al. Physical Review C, 1985, **31**: 74

13 Arthur E D, Young P G. Report of Los Alamos Scientific Laborator, 1980, Report No. LA-8626-MS (ENDF-304)

14 ZHANG Jing-Shang. The Statistical Theory for Neutron-Induced Light Reaction. Beijing: Science Press, 2009. 1(in Chinese)

15 SUN Xiao-Jun, QU Wen-Jing, DUAN Jun-Feng et al. Physical Review C, 2008, **78**: 054610-1

16 DUAN Jun-Feng, ZHANG Jing-Shang, WU Hai-Cheng et al. Physical Review C, 2009, **80**: 064612-1

17 QU Wen-Jing, LIU Ji-Feng, SUN Xiao-Jun. Chinese Physics C, 2009, **33**(1): 31

18 ZHANG Jing-Shang. Nucl. Sci. Eng, 1993, **114**: 55

19 ZHANG Jing-Shang, HAN Yin-Lu, CAO Li-Gang. Nucl. Sci. Eng, 1999, **133**: 218

20 ZHANG Jing-Shang. Nucl. Sci. Eng, 2002, **142**: 207

21 ZHANG Jing-Shang, YANG Xian-Jun. Zeitschrift für Physik A-Atomic Nuclei, 1988, **329**: 69

22 Chadwick M B, Oblozinsky P. Physcal Revew C, 1991, **44**: R1740

23 SHEN Qing-Biao. Nucl. Sci. Eng, 2002, **141**: 78

24 Kunz P D. Distorted Wave Code DWUCK4. University of Colorada, Boulder, Colorada, 1987